

Energy for connected objects

Electromagnetic energy harvesting and wireless power transfer



Student: Fatine Azzabi

Date: 09/10/2025

Student: Gabriel Benveniste

Student: João Gabriel Button Albuquerque

1 Introduction

The main goal of this lab is to show the possibility to turn on a red LED ROHM SML-D12U1WT8 only using electromagnetic energy transmitted via radio waves or within the energy available in the environment. We have two strategies to do that : direct consumption and store-then-use. The first one means that the LED is lightened up by the captured energy. The second approach is the store-then-use strategy in which the energy is firstly stocked in a supercapacitor through a power management unit (bq25504 + TPS63031) before getting used to lighten up the LED.

As an application context of this type of wireless power supply we can mention sensors integrated into the concrete intended for Structural Health Monitoring (SHM) for monitoring the structure's state. Indeed, in this type of environment, it is usually impossible to change/replace the batteries of the device, thus it's crucial to develop autonomous sensors able to power themselves through ambient energy, specially from RF waves from nearby transmitters.

Beyond powering a simple LED, this lab aimed to characterise the entire wireless power chain, from the rectifier and PMU to the antenna and to identify real-world limitations such as non-linear effects, MPPT behaviour, and polarisation influence.

The experiments were thus designed not only to validate the theoretical energy calculations but also to observe how component tolerances and propagation conditions affect the actual performance.

This LAB was divided into three parts:

1. LED & Power Budget : this part includes the calculation of the necessary power for turning on the LED and determining the feasibility of both strategies (direct and store-then-use).
2. Rectifier characterisation : we had to measure the performances of RF rectifiers at 868 MHz and 2.45 GHz and conclude on its efficiency, bandwidth and optimal charge.
3. Antenna choice : this last part was about comparing different antennas to select the more adapted one for one specific application.

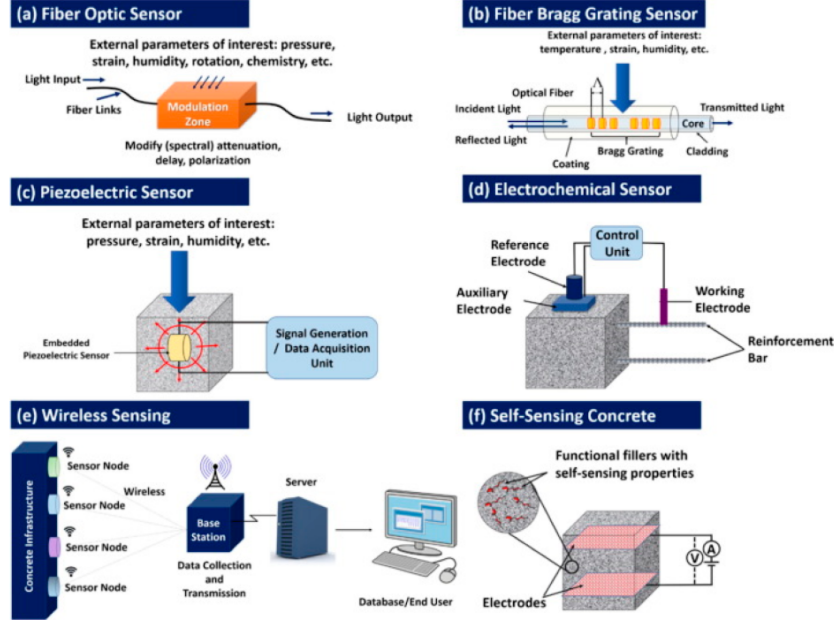


Figure 1: Example of an embedded sensor network for Structural Health Monitoring (SHM) in concrete
(source: MDPI Sensors, 2021)

Firstly, the energy harvesting consists of capturing a small amount of already present energy in the environment (such as light, heat, electromagnetic waves, vibrations...) and converting it into usable electricity. On the other hand, the wireless power transfer (WPT) relies on a wireless and contactless voluntary transmission of energy from a specific source toward a receptor.

Regarding the distance between the two, there can be either a nearby field transmission through an inductive or capacitive coupling (typically a few to several dozen centimetres, which corresponds to a short-range but still efficient transmission), or we can also have a distant field where the energy is transmitted through radiated electromagnetic waves, thus allowing it to reach several metres.

For our project, we're using radio frequency waves (RF) simply because they allow us to remote power supply while remaining compact and compatible with the ISM (Industrial, Scientific and Medical) bands at 868 MHz and 2.45 GHz, which are free to use. Hence, those frequencies range are a good option to have a nice range and efficiency but also a compact antenna size, which is what we are looking for when we are working with connected objects or integrated sensors (such as the one in concrete for the structure's following).

2 Theory

2.1 Power and Energy

The red diode that we will study in this lab is the *SML-D12V1W* from ROHM Semiconductors. From its datasheet table, useful information can be extracted (see highlighted content on Figure 1):

Ambient energy harvesting and wireless power transfer: focus on electromagnetic solutions

Near-field and far-field wireless power transfer				
Near-field		Far-field		
Capacitive coupling	Non-resonant inductive coupling	Resonant inductive coupling	Radiative (radiofrequency/microwave)	Laser
<ul style="list-style-type: none"> - Very short ranges - Very high voltages + Very good efficiency (>90 %) + Passes obstacles whose metal is insensitive + Misalignement insensitve + Little interferences ? Safety 	<ul style="list-style-type: none"> - Short ranges - Sensitive to metal - Sensitive to misalignement + Very good efficiency (>90 %) ? Safety 	<ul style="list-style-type: none"> - Short to medium ranges - Sensitive to metal - Sensitive to misalignement + Very good efficiency (>90 %) ? Safety + SWIPT 	<ul style="list-style-type: none"> + Large ranges + Good efficiency - Line of sight required - Interferences - Maturity - Electromagnetic compatibilities ? Safety + SWIPT 	<ul style="list-style-type: none"> + Very large ranges + Decent efficiency - Line of sight required - Interferences - Maturity ? Safety + SWIPT

Gaël LOUBET (gael.loubet@laas.fr) Energy for Connected Objects 77 / 133

Figure 2: Principle of wireless power transfer in near and far field (5ISS course - Energy for IoT)

■ Specifications																		
Part No.	Chip Structure	Emitting Color	Absolute Maximum Ratings (Ta=25°C)						Electrical and Optical Characteristics (Ta=25°C)									
			Power Dissipation P _D (mW)	Forward Current I _F (mA)	Peak Forward Current I _{FP} (mA)	Reverse Voltage V _R (V)	Operating Temp. T _{opt} (°C)	Storage Temp. T _{stg} (°C)	Forward Voltage V _F Typ. (V)	Reverse Current I _R Typ. (mA)	Max. (mA)	V _R (V)	Dominant Wavelength λ _D Min.*2 (nm)	Max.*2 (nm)	I _F (mA)	Luminous Intensity I _V Min. (mcd)	Typ. (mcd)	I _F (mA)
SML-D12V1W	AlGaN/P	Red	54	20	100*1	5	-40 ~ 85	-40 ~ +100	2.2	20	10	5	625	630	635	25	40	20
SML-D12U1W		Orange											615	620	625	40	63	
SML-D12D1W		Yellow											602	605	608	587	590	593
SML-D12Y1W		Yellow-green											569	572	575	16	30	
SML-D12M1W																		

*1:Duty1/10, 1kHz *2:Measurement tolerance: ±1nm

Figure 3: Specifications for SML-D12x1 Series, ROHM Semiconductors

- **Forward current rating** $I_F = 20mA$ (continuous).
- **Forward voltage** (typical) at $I_F = 20mA$: 2.2V
- **Power dissipation limit** $P_D = 54mW$

Note that conditions (current, voltage) to obtain this power dissipation limit are not displayed in the datasheet.

The electrical DC power can be expressed as $P = I_F \cdot V_F$, and the energy for 1 second as $E = P \cdot t$. Operating points can be extracted from the datasheet graphics (see Figure 2):

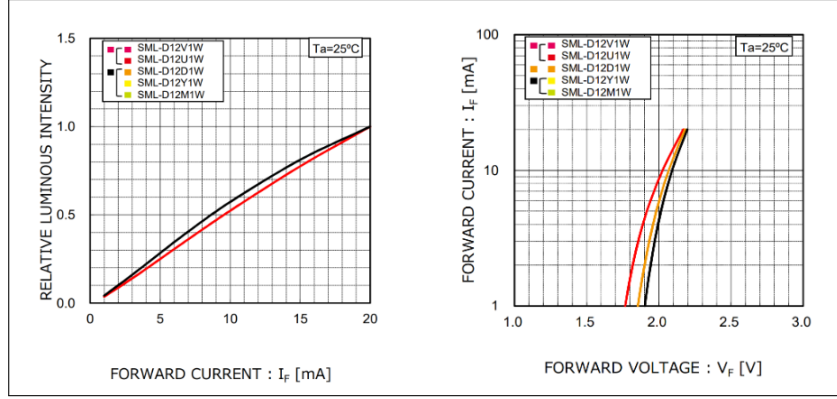


Figure 4: Luminous Intensity - Forward Current (Left), Forward Current - Forward Voltages (Right)

Theoretical results obtained from the data-sheet, can be merged into the following table:

Brightness (%)	Power (mW)	Energy (mJ)
100	44	44
50	19	19
25	9	9

Table 1: Power and Energy for the LED, different luminous intensities

Note that brightness and power (or energy) are not proportional, since luminous intensity vs current is not linear (but close) and the same applies to current vs voltage.

2.2 Consumption strategies

To light up the LED for *1 second*, two strategies can be used: lighting the LED directly from the rectifier (**direct**), or accumulating energy and then driving the LED at a controlled voltage/current (**store-then-use**).

- With **direct consumption**, the chain is quite simple: antenna → rectifier → LED. The response is immediate, but the LED current and brightness depend on the instantaneous RF field. The wave intensity also depends on the distance between the device and the power source (antenna). Because the power propagation is in a "donut" format, the farther the device is from the source, the less energy it receives. To ensure that the LED has a specific brightness for a specific amount of time, the ideal setup must store the minimal energy to power the LED for 1 second as wanted.
- With **store-then-use** (PMU + DC-DC + supercapacitor), the chain contains more elements: antenna → rectifier → PMU (*bq25504 PMU*) → storage (supercapacitor) → buck-boost (*TPS63031*) → LED. This system accumulates energy until there is enough to run the LED at a fixed current/-voltage. Factors such as cold-start, activation and deactivation voltage thresholds, and maximum capacitor losses must be considered (see §2.3).

The Power Management Unit (TI BQ25504) defines two thresholds: $V_{min} = 2.2 \text{ V}$ and $V_{max} = 5.25 \text{ V}$. It performs a Maximum Power Point Tracking (MPPT) routine every $\sim 14 \text{ s}$ by sampling the open-circuit voltage and adjusting its input impedance to about 40% of V_{oc} . This periodic sampling explains the voltage oscillations observed later in the experimental measurements.

2.3 Supercapacitor options

A capacitor stores energy $E = \frac{1}{2} \cdot C \cdot V^2$. A Power Management Unit (PMU) allows a discharge down to V_{min} and a charge up to V_{max} . The stored energy per cycle is called the usable energy:

$$E = \frac{1}{2} \cdot C(V_{max}^2 - V_{min}^2).$$

Since those threshold values and the stored energy are known, as seen in the previous section, it is easy to choose the right capacitor. For example, to store $44mJ$ at normal brightness with the given thresholds, the necessary capacitor has a value of $C = 3.9mF$. This capacitor is not on the given list of available capacitors, so the following one is taken, at $6.8mF$. If a bigger capacitor is chosen, thresholds must be adjusted to ensure that the equation remains valid.

How to fix V_{min} and V_{max} then? Since there is more energetic depletion with a higher voltage, the best way is to fix those thresholds as low as possible to reduce depletion. By doing so for each case (100%, 50% and 25%), the following table is obtained:

Brightness (%)	Energy (mJ)	Capacitor (mF)	Thresholds (V)	Max. losses (μW)
100	44	6.8	2.2 - 4.2	70
50	19	2.2	2.2 - 4.8	650
25	9	1.5	2.2 - 4.1	430

Table 2: Capacitor values

Note that these choices keep the discharge floor as low as the PMU allows ($2.2V$) to maximise usable ΔV^2 . Plus, max losses for each capacitor are not proportional to the amount of energy stored. They depend on capacitor technology (electro-lytic, electrochemical...).

It was observed that energy stored below V_{min} cannot be used by the PMU, resulting in “dead” energy. Larger capacitors store more total energy but also increase the charging time and the amount of unused energy. During the lab, the 6.8 mF capacitor required significantly longer to reach V_{max} than the 1.5 mF one, confirming this trade-off.

2.4 Rectenna fundamentals

In radiative WPT/RF harvesting the receiver is a rectenna. That is an antenna that captures RF power, an impedance-matching network that maximises power transfer, a non-linear rectifier (diode/transistor) that converts RF to DC, and a DC smoothing/storage stage. Co-optimising these blocks is essential. Note that the “best” antenna and the “best” rectifier in isolation do not yield the highest end-to-end efficiency together.

Selection is made by the operating band (868 MHz or 2.45 GHz in ISM), bandwidth, gain/pattern (omni vs directional), size, input impedance, and polarisation match to the transmitter.

The antenna type and polarisation have a direct influence on the harvested power. Linear-polarised antennas are sensitive to alignment: a 90° rotation between transmitter and receiver reduces the received power roughly by 50%. Circularly-polarised antennas would mitigate this effect in multipath environments. In this lab, both 868 MHz and 2.45 GHz bands were investigated.

3 Experiments

In the previous sections we've studied the architecture configuration for each energy objectives, 100%, 50% and 25% brightness. Our group was randomly provided with a "white box" device containing a 2.2 nF capacitor. Based on the previous studies (results of Table 2), we can deduct that it corresponds to the 50% brightness LED configuration. With this device in hands, our goal is to characterise the optimal rectifier frequency of this device, in order to identify its operating behaviour and the wireless power frequency, so we can see in witch frequency the device is more efficient wireless charging.

In this context, we are going to connect two devices to the board under study. One of this devices will act as a transmitter, sending energy at various frequencies, while the other will be used to observe the signal after the rectifier, showing the energy (in volts) obtained from the signal. Because we are working in high frequencies ($> 2\text{ GHz}$), we are not able to use a normal oscilloscope to observe the signal, for example, we need a more specific device. In a specific case like this, involving high frequencies and without using expensive equipment, our group was provided with the Ettus USRP B200 mini and the Analog Discovery 3, both connected to a Raspberry Pi 4, which is responsible for running the specific software required to control each device, GNU Radio and WaveForms respectively. The resulting experimental setup is illustrated in Figure 3.

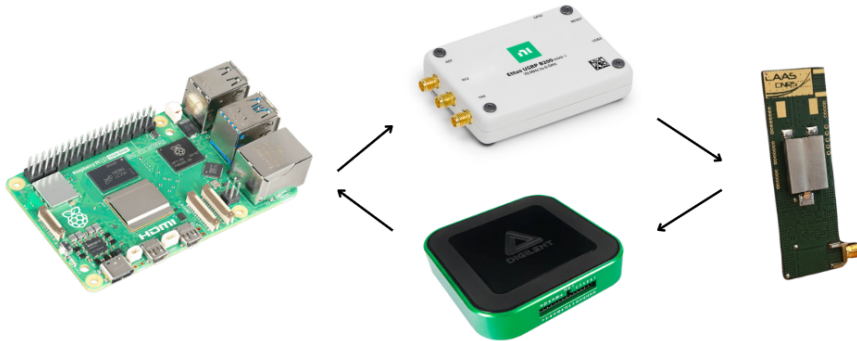


Figure 5: Experimental setup architecture

For this initial study, we are not going to use an antenna to send the energy signals. Because we are doing an initial frequency studies, we need the input signals to be as clean as possible and in the frequency that we want to study. This means that we don't want parasite ambient frequencies, for example, we want very efficient transfer of power from the source to the device. To do so, we've connected the Ettus USRP B200 Mini to the device in study with RF coaxial cable, which is similar to an fiber optic cable that directs the signal to the device.

The load was fixed at $1.5\text{ k}\Omega$ and the RF input power at 15 dBm (corresponding to a USRP gain of 73). Each frequency point was held for $\sim 16\text{ s}$ to allow the MPPT routine to stabilise before recording the voltage. All connections were first made through coaxial cables to eliminate parasitic effects, antennas were used later for over-the-air tests.

In the first 2 experiments, the Ettus USRP B200 Mini is used to generate the desired signal while performing a frequency sweep between 800 MHz and 950 MHz, and between 2.4 GHz and 2.5 GHz, with a frequency step of 10 MHz. The signal is applied to a resistive load of $1.5\text{ k}\Omega$ with an RF input power of -15 dBm , corresponding to a 74 gain in GNU Ration. Using the Analog Discovery 3, we are able to analyse the resulting energy signals after the rectifier. This experiments gives the results showed in Figures 4 and 5.

Furthermore, to evaluate the system's response over a broader frequency range and verify whether the device is optimised only for the target bands, or if it also harvests energy at other frequencies, we extended the sweep from 70 MHz to 3 GHz with a step of 100 MHz. This third experiment gives the results showed in Figure 6.

In the final part of the session, coaxial links were replaced with antennas in order to characterise the influence of radiation, distance, and polarisation on the harvested energy.

4 Results and discussions

In this section we are going to take a look at the results of each experiment and analyse the corresponding curves / signal outputs seen in WaveForms that correspond to the energy obtained for each frequency. Also discussing the conclusions of each signal response.

4.1 Experiment 1: 800 MHz to 950 MHz, step of 10 MHz

We can see in Figure 4 that the curves obtained in the experiment shows that we have a decreasing energy gain in relation to the frequency. If our device had been designed to operate at 868 MHz, we should have seen a increase of obtained power neat this frequency. We can also consider that the device is not perfect and the working frequency might have changed / dislocated to a smaller frequency (because we have more power in smaller frequencies).

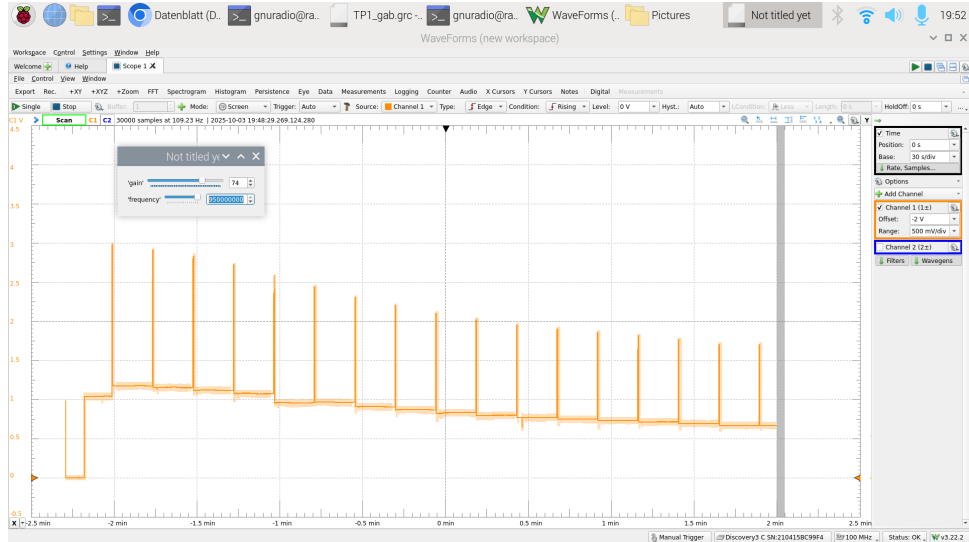


Figure 6: Experiment 1: 800 MHz to 950 MHz

4.2 Experiment 2: 2.4 GHz to 2.5 GHz, step of 10 MHz

We can see in Figure 5 that the power obtained in this range of frequency is bigger then the one obtained in the previous experiment and also that it's a steady curve. This means that we've found the optimal wireless charging frequency of the device, where it can obtain more power then 868 MHz with the same gain. Also that we've a range of frequencies that we can charge our device, with we'll see more clearly in the results of the next experiment.

Periodic fluctuations of the measured voltage (every ~ 14 s) were observed, corresponding to the MPPT open-circuit sampling described earlier.

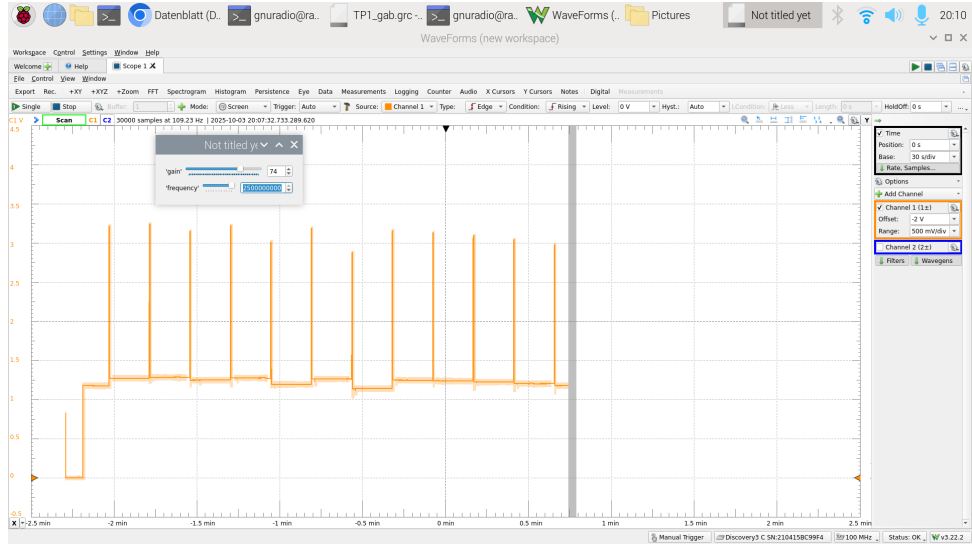


Figure 7: Experiment 2: 2.4 GHz to 2.5 GHz

4.3 Experiment 3: 70 MHz to 3 GHz, step of 100 MHz

If 868 MHz or 2.4 GHz were the ideal frequency, we would expect to see a band-pass behaviour around this frequencies, with a bigger amplitude. We can see this behaviour more clearly and with a bigger amplitude, meaning more energy received, in the 2.4 GHz frequency band. So we can conclude that our was built to work on this frequency. Even though the device was built to work on a specific frequency range, parasitics elements, coupling effects and non-linearities cause other frequencies to influence its overall behaviour.

The shift of the resonance peak when changing the input power confirms the non-linear behaviour of the diode rectifier. Component tolerances and PCB parasitics also contribute to these small frequency shifts.

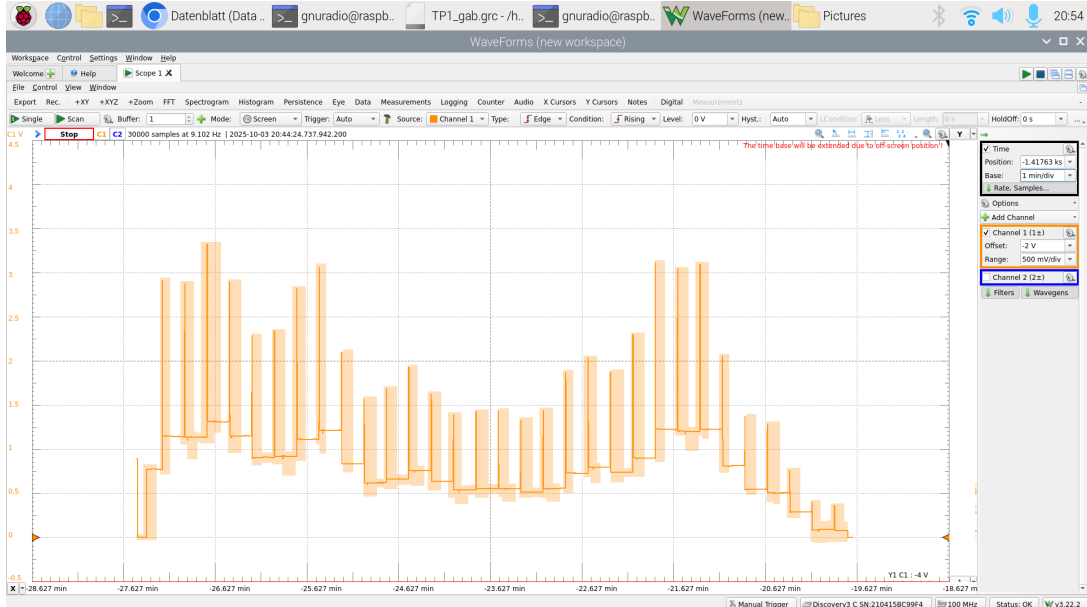


Figure 8: Experiment 3: 70 MHz to 3 GHz

4.4 Antenna and Polarisation Effects

After the coaxial characterisation, the system was tested over-the-air using 868 MHz and 2.45 GHz antennas.

At equal transmitted power (-15 dBm), the 2.45 GHz horn antenna provided the highest rectified voltage, while the 868 MHz patch showed lower output due to narrower bandwidth.

Rotating the receiving antenna by 90° reduced the rectified voltage by about half, confirming the sensitivity to polarisation alignment. The vertical orientation was more stable indoors, whereas the horizontal one suffered from reflections and depolarisation.

These results underline that antenna gain, alignment, and polarisation are key parameters in wireless power transfer efficiency.

4.5 MPPT Behaviour and Power Variation

The BQ25504 PMU periodically interrupts its input every $\sim 14 \text{ s}$ to sample V_{OC} (Voltage open circuit) and sets the operating point at 40% V_{OC} . This explains the voltage oscillations observed on the oscilloscope.

When the available RF power dropped below -18 dBm , the PMU could not start, defining the minimum power required for cold-start operation.

4.6 Ambient Harvesting and Wireless Power Transfer

This part of the work was not carried out during the lab due to time limitations. However, the instructor explained that ambient electromagnetic power levels are far too low to power a LED directly.

In practice, only a dedicated transmitter placed very close to the receiver can provide enough energy.

During the experiments, we observed that the LED could only turn on when the distance to the source was within a few tens of centimetres, confirming that ambient harvesting alone is not sufficient for this kind of application.

5 Conclusion

This lab demonstrated the complete characterisation of a wireless power transfer chain for low-power IoT applications.

Both direct consumption and store-then-use modes were validated, confirming theoretical energy requirements of 44 mJ, 19 mJ and 9 mJ for 100 %, 50 %, and 25 % brightness respectively.

The rectifier performed best near 2.45 GHz, showing a wide operating plateau, while the 868 MHz version delivered lower output.

The MPPT routine of the BQ25504 ($P \sim 14$ s cycle at 40 % V_{OC}) was clearly observed. Antenna alignment and polarisation strongly affected received power, a 90° rotation causing roughly 50 % loss.

These results confirm that the performance of wireless power transfer systems depends as much on circuit design as on antenna parameters and environmental conditions.

Future improvements could include circularly-polarised or dual-band antennas, adaptive matching networks, and optimised supercapacitors to extend range and stability.